

Time-resolved evolution of coherent structures in turbulent channels: Characterization of eddies and cascades

Supplementary material

By **Adrián Lozano-Durán** and **Javier Jiménez**

School of Aeronautics, Universidad Politécnica de Madrid, 28040 Madrid, Spain

(23 September 2014)

Appendix A. Details and validation of the tracking method

A.1. Spurious connections and branches

This appendix expands the discussion about the tracking method detailed in section 3. For all the results presented in the paper, those branches in which none of the structures attain a volume higher than 20^3 wall units are discarded to avoid grid resolution issues. Besides, branches which cross the edges of the temporal domain are dismissed since their histories are incomplete.

In order to remove spurious connections, four particular cases are corrected (see figure 1). Sometimes the branches do not clearly split or merge but they rather touch each other as shown in figures 1(*a,b*). In these cases, the connection between both branches is dismissed when the difference of volume between the structures labelled as (1) and (2) is less than 5% (figure 1*a*). On the other hand, the structures (1) and (2) are disconnected when such difference is larger than 90% (figure 1*b*). The same corrections are applied to the cases obtained reversing the time in figures 1(*a,b*). The third case is sketched in figure 1(*c*). When the beginning and the end of a branch belong to the same branch, it is considered that both represent the evolution of a single coherent structure and, hence, are gathered together as a single branch. The last correction is done when two branches are connected with the same node of a third branch as shown in figure 1(*d*). In this case, the first two branches are disconnected from the third one and reconnected together to form a single branch. The modification is applied only when the difference of volumes as well as the difference of the y - z centres of gravity of (1) and (2) are less than 10%. All the percentages given above are computed with respect to the largest magnitude involved.

Finally, we address the effect of the spatial shifting of the structures employed in the tracking step. As explained in section 3, in order to maximize the connections between structures at contiguous times t_n and t_{n+1} , the points of the objects at time t_{n+1} are shifted by a distance $-U(y)\Delta t_s$ in the streamwise direction. This may lead to spurious connections, especially between small structures. Most of the results presented in the paper were also computed without applying the shifting for case M950 and no important differences were observed. Some results are shown in table 1. Almost the same amount of branches and graphs are obtained, and the main consequence of removing the shifting is to increase the number of isolated structures, although their total volume remains negligible compared with the total volume of the non-isolated ones. The ratio between the amount of direct and inverse cascades, as defined in section 6.2, changes roughly by 3%.

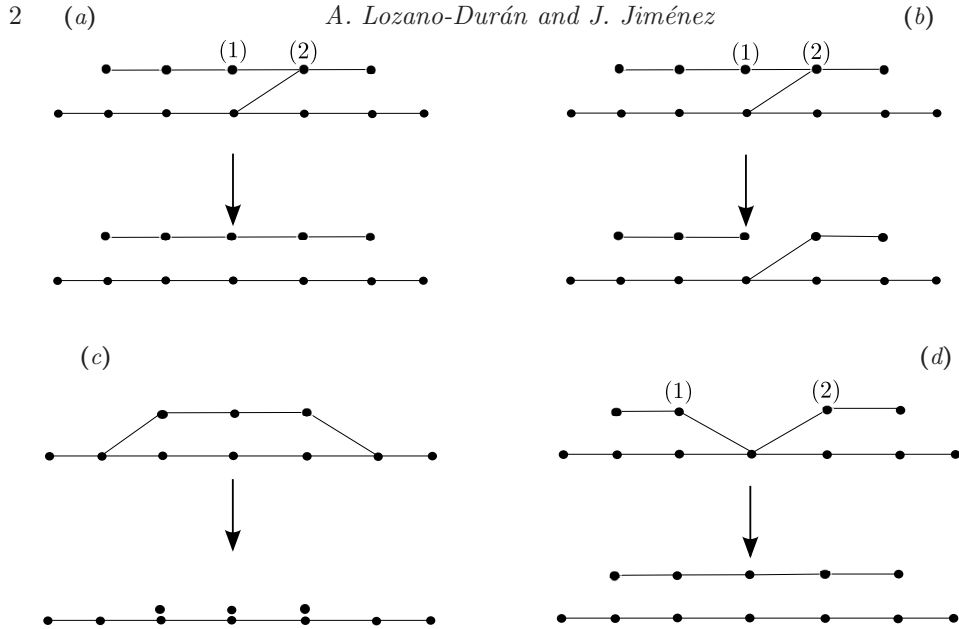


FIGURE 1. Sketches of the four types of connections corrected. For each graph, time is going from left to right. (a) Case I: two branches touch each other. The contact between them is dismissed. (b) Case II: two branches touch each other. One branch is disconnected in two. (c) Case III: a branch begins and ends at the same branch. Both of them are grouped into a single one. (d) Case IV: two branches are connected backward and forward with a third one at the same node. The two branches are disconnected and linked together to form a new one. See text for details of when the corrections are applied.

A.2. Validation of the tracking method

In order to verify that the tracking method is properly working, graphs and branches extracted from the actual turbulent flow were visualized (see, for instance, figure 5(a)). In addition, three tests were performed with synthetic data. They are shown in figure 2 which also includes the corresponding graphs. The first test consists of three eddies moving in the streamwise direction with different advection velocities. The second test is an initial eddy that first splits into two fragments of different sizes, then, each of them split again following the same process and finally all the objects merge in reverse order. The third test does not have any physical meaning and it is intended to check rare connections. All the cases were correctly captured by the tracking method.

To discard any bias of the method related to the arrow of time, Q graphs and branches were computed with data from case M950 that had been previously reversed in time. The results are as expected and are shown in table 1. The same number of branches and graphs are obtained, and the role of mergers and splits is exchanged, as it is supposed to happen.

Appendix B. Effect of the threshold and of the time step

Two new cases derived from M950 are defined to study the effect of the threshold and the time step between fields stored. The parameters are summarized in table 2. For case Ms950 the threshold H is almost doubled and for case Mt950 the time step is increased roughly by a factor of four. All the results presented in the paper were recomputed for cases Ms950 and Mt950 and no significant differences appeared. Some results are collected in figures 3(a,b,c,d) and table 2. The number of branches and graphs decreases for cases

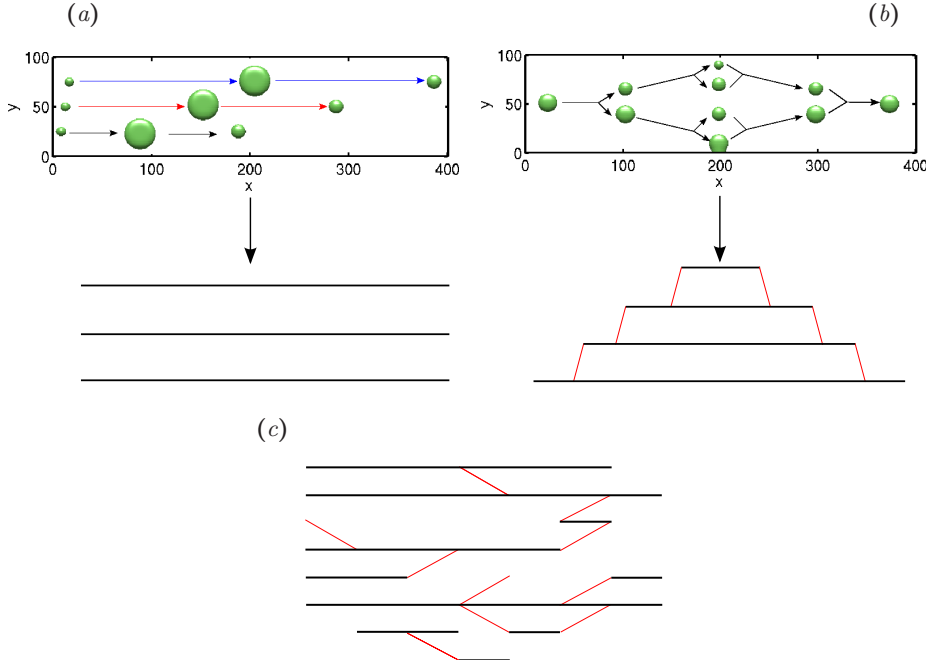


FIGURE 2. Artificially made test cases in arbitrary units. (a) Three objects moving with different advection velocities. (b) Objects splitting and merging. (c) Test with no physical meaning intended to check rare connections. For (a) and (b) the top figure shows the structures (in green) at different times (linked with arrows). The view is a x - y plane. The flow and time are going from left to right. The bottom part shows the corresponding graph with black lines for branches and red lines for mergers and splits. In case (c) only the graph is shown.

Case	N_B^Q	N_G^Q	N_S^Q	N_M^Q	N_I^Q	V_I^Q/V_T^Q	r_B
M950	3148888	1805427	570440	415147	153440	2.5×10^{-5}	1.21
M950 <i>time-reversed</i>	3148888	1805427	415147	570440	153440	2.5×10^{-5}	0.83
M950 <i>no shifting</i>	3154002	1825554	554322	398813	427059	1.6×10^{-4}	1.25

TABLE 1. N_B^Q , number of branches; N_G^Q , number of graphs; N_S^Q , number of mergers; N_M^Q , number of splits; N_I^Q , number of isolated structures; V_I^Q/V_T^Q , ratio between the total volume occupied by isolated objects and volume of all the objects; r_B , ratio between the amount of direct and inverse cascade as defined in section 6.2. Data for Qs. The results presented in the paper correspond to case M950. Case M950 *time-reversed* is case M950 with the arrow of time reversed. Case M950 *no shifting* is case M950 but without shifting the structures a distance $-U(y)\Delta t_s$ in the streamwise direction before computing their connections.

Ms950 and Mt950, although the total volume of isolated structures remains smaller than 0.01% with respect to the total volume of objects. Maybe, the most remarkable change is an increase of 10% in the ratio between the amount of direct and inverse cascades for intense Q⁻s with $H = 3$ compared to those computed with $H = 1.75$. Figure 3(a) shows that coarsening the time between fields stored does not affect the statistical trends of tall attached branches, and its effects are only visible for detached and buffer layer branches whose lifetimes are close to the temporal resolution limit. Sizes and advection velocities

Case	H	Δt_s^+	N_B^Q	N_G^Q	N_I^Q	V_I^Q/V_T^Q	r_B	Symbol
M950	1.75	0.8	3.15	1.81	0.15	2.5×10^{-5}	1.21	none
Ms950	3.00	0.8	1.79	0.91	0.09	4.1×10^{-5}	1.32	□
Mt950	1.75	3.8	1.38	0.82	0.21	1.07×10^{-4}	1.24	×

TABLE 2. Summary of the parameters and results from case M950 and the sub-cases derived from from it. H , threshold parameter as defined in section 2.2; Δt_s , time step between fields stored; N_B^Q , number of branches; N_G^Q , number of graphs; N_I^Q , number of isolated structures. All numbers are in millions. V_I^Q/V_T^Q , ratio between the total volume of isolated objects and volume of all the objects; r_B , ratio between the amount of direct and inverse cascade as defined in section 6.2. Data for Qs.

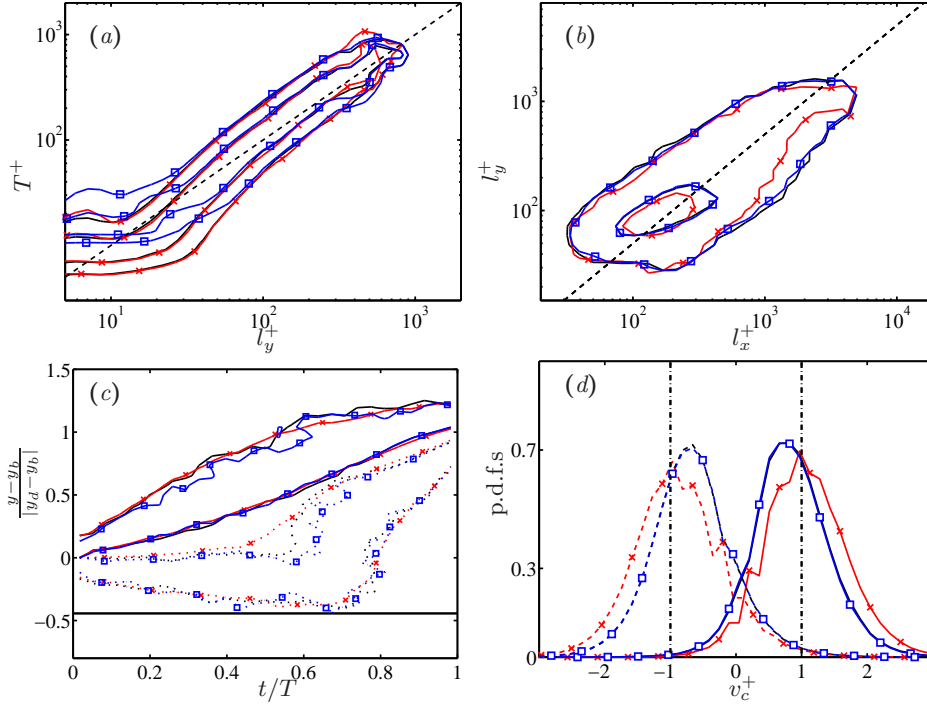


FIGURE 3. (a) P.d.f.s of the lifetimes of Q^- s primaries as a function of the wall-normal length of the branch, l_y . Each vertical section is a p.d.f. Contours are 40% and 80% of the maximum. The straight dashed line is $T^+ = l_y^+$. (b) Joint p.d.f.s of the logarithm of the streamwise, l_x , and wall-normal, l_y , sizes of tall attached primaries. Data for ejections. The dashed straight line is $l_x = 2l_y$. Contours are 50% and 98% of the data. (c) P.d.f.s of the minimum (---) and maximum (—) heights of tall attached primary branches, as functions of the time elapsed from their birth. Time is normalized with the lifetime of each branch, T , and y_{min} and y_{max} with the heights, y_b and y_d , at its birth and death, respectively (see figure 10 in the paper). The solid horizontal lines are the average position of the wall. (d) P.d.f.s of the wall-normal velocity of the centre of gravity of sweeps (---) and ejections (—). The vertical dashed-dotted lines are $v_c = \pm u_\tau$. Symbols as in table 2.

are qualitatively similar. More thresholds were tested without any remarkable change for Qs defined within $1.25 < H < 3$. A similar threshold analysis was performed for vortex clusters with no important differences for $0.01 < \alpha < 0.04$.